Antibodies to protozoan variable surface antigens induce antigenic variation

Albano H. Tenaglia[1,2]*[§], Lucas A. Luján[1,2]*, Diego N. Ríos[1,2]*, Victor Midlej[3,4], Paula A. Iribarren[5], Cecilia R. Molina[1,2], M. Agustina Berazategui[5], Alessandro Torri[1§], Alicia Saura[1,2], Damián O. Peralta[1], Macarena Rodríguez-Walker[1,7], Elmer A. Fernández[1,7], Juan P. Petiti[8], Marianela C. Serradell[1,9], Pablo R. Gargantini[1,2], Vanina E. Alvarez[5], Wanderley de Souza[3], Hugo D. Luján[1,2]

[1]Centro de Investigación y Desarrollo en Inmunología y Enfermedades Infecciosas (CIDIE), Consejo Nacional de Investigaciones Científicas y Técnicas (CONICET)/Universidad Católica de Córdoba (UCC). X5016HDK. Córdoba, Argentina.
[2]Facultad de Ciencias de la Salud, Universidad Católica de Córdoba (UCC). X5016HDK. Córdoba, Argentina.
[3]Intituto de Biofísica Carlos Chagas Filho and Centro Nacional de Biologia Estrutural e Biomagens (CENABIO), Universidade Federal do Rio de Janeiro (UFRJ). 21941-170. Rio de Janeiro, Brazil.
[4]Instituto Oswaldo Cruz, Fundação Oswaldo Cruz (FIOCRUZ). 21040-900. Rio de Janeiro, Brazil.
[5]Instituto de Investigaciones Biotecnológicas (IIBIO), Consejo Nacional de Investigaciones Científicas y Técnicas (CONICET)/Universidad Nacional de General San Martín (UNSAM). B1650HMP. Buenos Aires, Argentina.
[7]Facultad de Ingeniería. Universidad Católica de Córdoba. X5016HDK. Córdoba, Argentina.
[8]Instituto de Investigaciones en Ciencias de la Salud (INICSA), Centro de Microscopía Electrónica, Facultad de Ciencias Médicas. CONICET/Universidad Nacional de Córdoba. X5016HUA. Córdoba, Argentina.
[9]Laboratorio de Parasitología y Micología, Departamento de Bioquímica Clínica, Facultad de Ciencias Químicas, Universidad Nacional de Córdoba. X5016HUA. Córdoba, Argentina.

*These authors contributed equally to this work.

[§]Present address: Alessandro Torri, Viruses and RNA Interference Unit, CNRS Unité Mixte de Recherche, Institut Pasteur. Paris. France.

[§]Present address: Albano H. Tenaglia, Antibody and Vaccine Group, School of Cancer Sciences, University of Southampton Faculty of Medicine. Southampton. UK.

[§]Present address: María A. Berazategui, Department of Life Sciences, Sir Alexander Fleming Building, Imperial College London, London, UK.

Abstract

The genomes of most protozoa encode families of variant surface antigens, whose mutually exclusive changes in expression allow parasitic microorganisms to evade the host immune response[1,2]. It is widely assumed that antigenic variation in protozoan parasites is accomplished by the spontaneous appearance within the population of cells expressing antigenic variants that escape antibody-mediated cytotoxicity[1,2]. Here we show, both *in vitro* and in animal infections, that antibodies to Variant-specific Surface Proteins (VSPs) of the intestinal parasite *Giardia lamblia* are not cytotoxic, inducing instead VSP clustering into liquid-ordered phase membrane microdomains that trigger a massive release of microvesicles carrying the original VSP and switch in expression to different VSPs by a calcium-dependent mechanism. Surface microvesiculization and antigenic switching are also stimulated when *Trypanosoma brucei* and *Tetrahymena thermophila* are confronted to antibodies directed to their GPI-anchored variable surface glycoproteins. This novel mechanism of surface antigen clearance throughout its release into microvesicles coupled to the stochastic induction of new phenotypic variants not only changes the current paradigm of spontaneous antigenic switching but also provides a new framework for understanding the course of protozoan infections as a host/parasite adaptive process.

Main

Antigenic variation (AV) is a mechanism developed by parasitic microorganisms to change the expression of their highly immunogenic surface molecules[1]. AV was discovered more than a century ago[2] and is considered an intrinsic process responsible for persistent and recurrent infections caused by unicellular microorganisms[1-3].

Giardia lamblia colonizes the lumen of the upper small intestine of vertebrates[4]. Its life cycle includes the environmentally resistant cysts and the proliferating trophozoites, which attach to the gut surface and cause the clinical manifestations of giardiasis[4]. Unlike other protozoan parasites, AV in *Giardia* was discovered as a phenomenon occurring *in vitro*[5] (i.e., in the absence of any immune pressure) before being found to occur during animal infections[6], suggesting that spontaneous antigenic switching is an inherent characteristic of this parasite.

AV in *Giardia* involves VSPs, which cover the entire trophozoite surface and are the main antigens recognized by their hosts[4-7]. VSPs are integral membrane proteins with antigenically variable ectodomains containing multiple CXXC motifs and a highly conserved C-terminal region, comprising a transmembrane domain (TMD) and a short cytoplasmic tail (CT)[7-9]. The parasite genome encodes a repertoire of 136 VSPs[9], but only one is expressed on the surface of individual trophozoites at any time[8]. Expression of a unique VSP is regulated post-transcriptionally by an RNAi-like mechanism and maintained epigenetically[10]. However, why and how trophozoites change one VSP for another remains unknown.

As a major host response, the effect of antibodies against surface antigens has basically been studied in terms of their fate after binding to the cell surface. Many protozoa cope with surface-adhered antibodies by either segregating them into "caps" or transferring the antigen/antibody complex to a "flagellar pocket" for endocytosis and lysosomal degradation, thereby avoiding protozoan agglutination and opsonization[11-14]. If antibody concentrations exceed the capability to

2

79   remove them, parasites might die by either complement-dependent or independent antibody-
80   mediated cytotoxicity[11-16]. Similarly, antibodies against *Giardia* VSPs have extensively been
81   reported to be cytotoxic[6,15-19].

82   AV takes place at very low rates in *Giardia* cultures[4,16] and does not seem to occur in antibody-
83   deficient hosts[4,8]. During the course of infections in immunocompetent individuals, however, if
84   antibody-mediated killing is as efficient as it was found *in vitro*, the number of switchers should
85   be too low to sustain chronic infections. Therefore, we hypothesized that the relationship
86   between protozoan parasites and the host immune response is more complex than previously
87   speculated and that antibodies play a major role during AV.

88

Antibodies to VSPs stimulate switching

90   *Giardia* isolates are arranged into genetic groups or assemblages, each having a particular VSP
91   repertoire[7-9]. When *Giardia* trophozoites are exposed to anti-VSP monoclonal antibodies (mAbs)
92   or serum collected from infected animals, parasites agglutinate into large aggregates that have
93   been considered clusters of dead cells[6-8,17-19].

94   To better explore the effect of antibodies to VSPs, specific mAbs against VSPs from
95   trophozoites belonging to assemblages A1 (isolate WB/C6) and B (isolate GS/M-83) (**Extended
96   Data Table 1**) were used to select by limiting dilution *Giardia* clones expressing either VSP417,
97   VSP1267 or VSPH7. Once cloned (**Extended Data Fig. 1a**), trophozoites were confronted to
98   different concentrations of their specific anti-VSP antibody. Results showed that at high
99   concentrations (100 µM), purified mAbs produced the rapid detachment of the parasites from the
100   culture tubes and their clumping into aggregates containing live trophozoites, which remained
101   grouped but motile for days (**Extended Data Fig. 1b** and **Supplementary Movie 1**). When the
102   same clones were confronted for 72 h to lower concentrations of either their anti-VSP mAb or to
103   an unrelated mAb[20] (both at 50 nM), anti-VSP antibodies only produced a transient parasite
104   detachment and agglutination (**Extended Data Fig. 1c**), although neither their viability (**Fig. 1a**
105   and **Extended Data Fig. 1d**) nor proliferation (**Fig. 1b**) was affected. However, almost no
106   trophozoite in the anti-VSP antibody treated population maintained the expression of the original
107   VSP, unlike the controls (**Fig. 1c**), indicating that low concentrations of anti-VSP antibodies may
108   induce antigenic switching. Moreover, in clones treated with varying antibody concentrations
109   and for different periods, the percentage of switchers incremented with both increasing induction
110   time and antibody concentration (**Fig. 1e**). Since experiments were performed in clones
111   expressing different VSPs and using a variety of mAbs, the observed effects were not influenced
112   by either the isotype of the anti-VSP mAb or their potential differences in affinity (**Extended
113   Data Table 1**).

114   To determine whether the observed AV was caused by induction of switching or by
115   antibody-mediated negative selection, two different approaches were used. First, trophozoites
116   expressing a given VSP were re-cloned in culture medium already containing either the mAbs
117   directed to their specific VSP or the control antibody (50 nM). After 5 days, no differences in the
118   number of growing clones were found (**Extended Data Fig. 2**). Since clones originated from a
119   single trophozoite in contact with their anti-VSP mAb, the absence of antibody-induced killing
120   was confirmed. In the controls, most clones maintained their VSPs, whereas in antibody-treated
121   cells the number of trophozoites expressing the original VSP was particularly low (**Fig. 1d** and
122   **Extended Data Fig. 2**). Moreover, when the expression of different VSPs was examined by

123 immunofluorescence assays (IFAs), all these newly expressed VSPs were present in small
124 percentages, accounting for the absence of any order in the expression of the novel VSPs
125 (**Extended Data Table 2**). Second, the differences in switching rates between clonal populations
126 expressing VSP417 treated or not for 72 h with 50 nM of the anti-VSP417 mAb were evaluated
127 using an adapted Luria-Delbrück fluctuation test[21,22]. At these antibody concentration and
128 incubation time, results showed that anti-VSP antibodies induced a ~72-fold increase in the
129 switching rate as compared to the controls (**Extended Data Table 3**). Besides, the fluctuation[21]
130 (variance/mean value) was >100 higher in untreated cells than in clonal parasites treated with its
131 corresponding anti-VSP mAb, strongly supporting that AV is induced by antibodies.

132   To delve into the dynamics of VSP replacement, trophozoites expressing VSP417 were
133 grown in the presence of mAb 7C2 or of the unrelated mAb (50 nM). At different time points,
134 the number of trophozoites labelled with mAb 7C2 and a polyclonal antibody against VSPs other
135 than VSP417 (pAb VSP417$^{(-)}$) was determined by IFAs and flow cytometry. Results showed a
136 decrease of the number of cells expressing the original VSP over time, with the concomitant
137 increase of those simultaneously expressing the original and the novel VSPs, and finally cells
138 expressing only the new VSPs (**Fig. 1f, g**). Representative flow cytometry plots show that
139 control cells exhibited no changes over a 72-h period; in contrast, mAb 7C2-treated trophozoites
140 showed a conversion path from VSP417$^{(+)}$ to VSP417$^{(-)}$ cells throughout the treatment (**Fig. 1h**).
141 This exchange was better observed in three different VSP417-expressing *Giardia* trophozoites
142 incubated for 24 h with mAb 7C2, in which one is still expressing the original VSP, another has
143 already switched to the expression of a new VSP and the third parasite is still in process of
144 switching (**Fig. 1i**). This period of VSP colocalization clearly shows that there is no negative
145 selection; instead, there is a true exchange of the VSP on the trophozoite membrane.

146

Antibody-mediated VSP signalling

148 If antibodies against the different ectodomains of VSPs stimulated antigenic variation, VSPs
149 might signal throughout their highly conserved C-terminal region, which comprises the TMD
150 and a 5-amino acid CT (**Fig. 2a**).

151   Previous reports suggested the involvement of post-translational modifications of the
152 CRGKA tail of VSPs, such as Cys-palmitoylation and Arg-citrullination in antibody-mediated
153 cytotoxicity, and Lys-ubiquitination in VSP recycling[4,18,19]. Therefore, the influence of the CT of
154 VSPs during AV was evaluated in trophozoites simultaneously expressing two VSPs, which
155 share their conserved C-terminal region but differ in their ectodomains. Trophozoites of the
156 isolate WB endogenously expressing VSP417 were transfected to constitutively express the
157 VSPH7 of isolate GS/M-83 (with or without mutations in its CT) to function as "sensors" of the
158 anti-VSP antibody whereas VSP417 may serve as "reporter" of antigenic switching (**Extended
159 Data Fig. 3a**). Trophozoites co-expressing VSP417 and VSPH7 with and without CT variants
160 (**Extended Data Fig. 3b, c**) were then grown in the presence of mAb 7C2 to induce switching of
161 VSP417 and, separately, in the presence of mAb G10/4 to induce switching of VSP417 through
162 binding to VSPH7. After 72 h, mAb 7C2 promoted switching of VSP417 as expected, but mAb
163 G10/4 also induced switching of the reporter VSP417 in trophozoites co-expressing the VSPH7
164 wild type CT CRGKA as well as those having the CT variants <u>K</u>RGKA, C<u>A</u>GKA and CRG<u>AA</u>
165 (**Fig. 2b**). These results indicate that, despite its conservation, the short CT of VSPs is not
166 involved in signalling.

167   Consequently, the highly homologous TMD of VSPs was investigated. A high degree of
168   identity was found between TMD of VSPs and those of surface antigens of other protists (e.g.,
169   *Trichomonas* spp., *Spironucleus* spp. and *Leishmania* spp.) and that of the mammalian
170   carcinoembryonic antigen-related cell adhesion molecule 1 (CEACAM1)[23] (**Extended Data Fig.**
171   **3b**). The similarity included length and presence of G-xxx-G and small(L/I/V)-xxx-small(L/I/V)
172   motifs (GAS) and a domain rich in aromatic residues (ARO), all known to facilitate the
173   formation of dimers and high-order oligomers[23-25]. Therefore, these motifs were disrupted by
174   substituting the small amino acids of the TMD of VSPH7 for the larger amino acid Methionine
175   and, separately, the aromatic residues of were exchanged for Valines (**Extended Data Fig. 3b**).
176   Then, the effects of mAb G10/4 in parasites co-expressing VSP417 was analysed. Despite being
177   localized at the cell membrane (**Extended Data Fig. 3c**), TMD variants lacking either the GAS
178   motifs or the ARO domain notably diminished VSP417 switching induced by the anti-VSPH7
179   antibody (**Fig. 2c**). Since these mutations changed the capability of TMD oligomerization
180   (**Extended Data Fig. 3d**), results indicated that the TMDs of VSPs play an important role in
181   transducing the stimulus for AV.

182   In addition, since antibodies might facilitate VSP/VSP interactions, mAb 7C2 was
183   fragmented to its corresponding Fabs and their relative ability to induce VSP417 switching was
184   compared. Unlike the intact mAb (50 nM), Fab fragments (100 nM) failed to induce antigenic
185   switching, but their efficiency was restored when Fabs were clustered with secondary antibodies
186   (**Fig. 2d**), suggesting that VSP TMD oligomerization and VSP clustering are crucial for
187   switching.

188   TMD length and sequence are key determinants of liquid-ordered phase (l_o) membrane
189   microdomains association[26] and, indeed, CEACAM1 and oligomerized plasma membrane
190   proteins are usually present on lipid raft-like structures[23-26], as also are the GPI-anchored variable
191   surface antigens of other protozoa[1,27]. In *Giardia*, the characteristics of VSP TMD suggested that
192   they would also translocate into l_o-phase, lipid raft-like membrane domains, which were
193   previously described in this parasite[28]. In fact, when trophozoites were cultured in the presence
194   of 10 mM of methyl-β-cyclodextrin (MβCD, a cholesterol-rich microdomain disrupting agent),
195   VSP switching induced by anti-VSP mAbs was abolished (**Fig. 2d**). Hence, Triton X-100 lysates
196   of trophozoites expressing VSP417 pre-treated or not with 50 nM of mAb 7C2 for 1 h were
197   subjected to sucrose density gradient centrifugation to allow the isolation of low-density
198   detergent resistant membranes (DRM), which have properties of lipid rafts[29]. VSP417 was
199   mainly detected in detergent soluble membranes (DSM) in both treated and untreated
200   trophozoites, but a fraction of the VSP417/mAb 7C2 complexes redistributed into DRM upon
201   antibody binding. Notably, pre-treatment of trophozoites with 10 mM of MβCD before DRM
202   isolation avoided antibody-induced VSP417 redistribution into DRM (**Extended Data Fig. 4**).
203   These results are consistent with results of IFAs, which showed that at 1 h of incubation with the
204   anti-VSP antibody most of the VSP were still present all over the plasma membrane of the
205   trophozoites, whereas the VSP/antibody complex localized into punctate domains (**Fig. 2e**).
206   Therefore, the TMD of the VSPs may direct these proteins into cholesterol-rich microdomains
207   upon antibody binding. Since l_o-phase domains are dynamic structures, it is likely that VSP-
208   antibody interactions stabilize VSPs into larger platforms capable of recruiting cytoplasmic
209   molecules that activate signal transduction mechanisms[38].

210

211   **VSPs are removed into microvesicles**

5

212 To track the fate of the VSP bound to its specific antibody, *Giardia* clones expressing different
213 VSPs were treated with their corresponding mAbs and analysed by structured illumination
214 microscopy (SIM) 24 h post-induction (hpi). At the plasma membrane, the cognate VSP formed
215 clusters and the newly expressed VSP showed a more homogeneous distribution (**Fig. 2f**). These
216 microdomains were then studied at the ultrastructural level by combining transmission (TEM)
217 and scanning (SEM) electron microscopy with or without immunogold-labelling. In **Fig. 2g** and
218 **h,** immunogold TEM micrographs of a *Giardia* trophozoite at 30 mpi showed groups of
219 microvesicles (MVs) on their surface. By SEM, the cell surface changed from smooth in
220 untreated trophozoites (**Fig. 2i**) to rough, full of MVs in antibody-treated cells (**Fig. 2j**). SEM
221 with gold labelling showed that these MVs clumps were enriched in the target VSP (**Fig. 2k, l**).
222 In contrast to the current assumption that the former surface antigen disappear by its continuous
223 dilution in the plasma membrane after a new antigen is being expressed, these results indicate
224 that after antibody binding, VSPs are eliminated from the cell surface into extracellular MVs. In
225 this process, called "Antigen Removal Coupled to Switching (ARCS)", both surface antigen
226 clearance and antigenic variation are simultaneously triggered by surface antigen clustering into
227 lipid raft-like microdomains.

228 To test if a similar process occurs *in vivo*, gerbils (*Meriones unguiculatus*) were infected
229 with VSP417-expressing trophozoites and intestinal parasites were collected and analysed by
230 SEM and flow cytometry at different days post-infection (dpi). At the onset of the humoral
231 immune response (**Fig. 3a**), the same protrusions and MVs that were seen upon antibody
232 treatment *in vitro* were observed in trophozoites collected from the small intestine (**Fig. 3b, c**).
233 Moreover, conversion from VSP417$^{(+)}$ to VSP417$^{(-)}$ cells was observed between 10 and 12 dpi,
234 with a peak of original/new VSP co-labelling at 11 dpi (**Fig. 3d**). As observed *in vitro*, switching
235 to different VSPs within the intestine was random (**Fig. 3e**).

236 To determine the composition of the MVs, proteomic analysis (**Extended Data Table 4**) of
237 purified MVs collected 4 hpi (**Fig. 3F**) demonstrated that their most enriched molecule is the
238 original VSP. Except for multiple annexins (α-giardins[30]), ALIX/PDC6IP[31] and components of
239 the ESCRT machinery[32], most proteins found in the antibody-induced MVs (**Extended Data
240 Table 4**) were similar to *Giardia* MVs artificially generated by incubation of the parasites with 2
241 mM of extracellular calcium[33].

242 To test if antigenic variation can be triggered by the sole induction of MVs, clonal
243 trophozoites were incubated with different extracellular [Ca^{2+}] in either absence or presence of
244 anti-VSP antibodies. Neither viability nor proliferation was affected after 72 h of incubation,
245 except in the presence of high concentrations of EGTA (10 mM) (**Extended Data Fig. 5**), but
246 VSP switching was only induced when antibodies directed to their cognate VSP were present
247 (**Fig. 3g**). Conversely, the intracellular Ca^{2+} chelator BAPTA-AM (0.5 µM) suppressed
248 switching in trophozoites treated for 72 h with antibodies against their VSP (**Fig. 3g**), without
249 affecting parasite viability or proliferation (**Extended Data Fig. 5**). To determine if VSP
250 clustering by antibodies promotes an increase in the intracellular [Ca^{2+}], trophozoites expressing
251 VSP417 previously loaded with the calcium indicator Fluo 4-AM were subsequently incubated
252 with either mAb 7C2 or a control mAb (50 nM). Results showed a strong increase in the
253 intracellular [Ca^{2+}] soon after antibody binding to the VSP (**Fig. 3h**), in the presence or the
254 absence of extracellular Ca^{2+}. Remarkably, although the Ca^{2+} ionophore A23187 (10 µM) also
255 increased the intracellular [Ca^{2+}] to similar levels (**Fig. 3h**), it did not induce antigenic switching
256 (**Fig. 3g**). This result suggests that an intracellular Ca^{2+} increase is necessary but insufficient to

6

257 trigger ARCS and that the mechanical clustering of VSP caused by anti-VSP antibodies elicit a
258 more complex process responsible for antigen elimination and switching. Since Ca^{2+} is essential
259 for the function of annexins, ALIX/PDCD6IP and PDCD6/ALG-2 (**Extended Data Table 3**)
260 during plasma membrane repair, virus budding and signal transduction[34-36], these results suggest
261 that anti-VSP antibodies promote the discharge of Ca^{2+} from intracellular stores to promote
262 ARCS.

263

ARCS occurs in other protozoa

265 The fact that the TMD of VSPs makes these molecules raftophilic highlights the similarity to
266 other protozoan variable surface antigens that are attached to the plasma membranes by GPI
267 anchors[1,27,37]. Consequently, antibodies to *T. brucei* variant surface glycoproteins (VSGs) and *T.*
268 *thermophila* i-Antigens were generated and used to determine if a process similar to that found in
269 *Giardia* is also occurring in these protozoa.

270 In *T. brucei*, mouse anti-VSG antibodies generated during experimental infections were not
271 cytotoxic at high dilutions (>1/1,000) and turned the parasite smooth surface into one full of
272 nanotubes and MVs after antibody treatment (**Fig. 4a-f**). Since these morphological changes
273 were similar to those observed in *Giardia* trophozoites exposed to anti-VSP antibodies, the
274 connexion between cell membrane microvesiculation induced by anti-VSG antibodies and
275 antigenic switching was evaluated using two different procedures. First, an experimental method
276 was designed to test the influence of increasing concentration of anti-VSG antibodies on the
277 growth of *T. brucei* and to allow the identification of potential switchers (**Extended Data Fig.**
278 **6**). Briefly, three parallel cultures of parasites expressing VSG AnTat1.1 were grown for 72 h in
279 the presence of either preimmune serum or sub-lethal daily doses of the anti-VSG pAb. Then,
280 serial dilutions of each culture were spread over a 96-well plate and parasites were exposed to a
281 lethal dilution of the anti-VSG pAb (1/50) to kill non-switchers. After 6-8 days, wells containing
282 live parasites were subjected to cDNA sequencing for identification of switchers. Results
283 demonstrated that increasing concentrations of specific anti-VSG antibodies induce switching to
284 different VSGs without affecting proliferation of the parasites (**Fig. 4g**). Furthermore, while the
285 two clones that survived in the control expressed the same VSG, clones isolated from the
286 cultures treated with the anti-VSG pAb expressed a diversity of VSG (**Fig 4g**), confirming that
287 they indeed correspond to independent switching events. Second, to determine switching rates in
288 the presence or absence of anti-VSG pAb, an adapted Luria-Delbrück fluctuation test[21] was
289 performed using either lethal dilution of the anti-VSG antibody (1/50) or a well described *VSG*
290 RNAi strategy[22] for the selection of switchers. In these experiments, parallel cultures containing
291 a very low number of parasites were expanded for 8-9 generations in the presence of either anti-
292 VSG AnTat1.1 pAb (1/1,000) or the preimmune serum before cultures were spread over 96-well
293 plates for selection of switchers by using a lethal dilution of the anti-VSG pAb (1/50) or,
294 separately, by addition of doxycycline to induce *VSG* AnTat1.1 RNAi. Since *VSG* RNAi results
295 in cell-cycle arrest and subsequent death, only parasites that have switched to a new VSG variant
296 will be able to grow[22]. Using both approaches, the calculated switching rate of the parasites
297 treated with anti-VSG pAb increased 10-25 times as compared to the parasites incubated with the
298 control serum (**Extended Data Table 5a and b**). Furthermore, the variance in the number of

299 clones generated per culture divided by the mean resulted much closer to 1 in the presence of
300 anti-VSG pAb (**Extended Data Table 5a and b**), confirming that VSG switching is induced by
301 the anti-VSG antibodies.

302 Similar experiments were performed in clones of the free-living protozoan *T. thermophila*. High
303 dilutions (>1/1,000) of antibodies to their surface antigens generated a temporary agglutination
304 of the cells with the concomitant disappearance of the recognized antigen, which reappeared on
305 their surface several days after the antibody was removed from the culture (**Extended Data Fig.
306 7**). As in *Giardia* and *T. brucei*, SEM analysis showed that the surface of this ciliate appeared
307 decorated with clumps of MVs soon after antibody treatment (**Fig. 4h-j**), clearly denoting that
308 ARCS may be a widespread process in protozoa.

309

Discussion

311 Antigenic variation seems to occur sporadically in protozoan cultures, which was interpreted as a
312 spontaneous process that allows switching of surface antigens after a given number of
313 generations[1]. Unlike previously assumed[6,15-19], antibodies against variant surface antigens are not
314 cytotoxic at low concentrations; rather, they strongly stimulate antigenic switching. This is the
315 first description of a host-induced tuning of AV, with important consequences for understanding
316 the course of protozoan infections and the propensity for multiple reinfections.

317 Our findings show that variable surface antigens acquire the role of sensors of the humoral
318 immune response, promoting antibody-directed phase separation of antigens into l_o-phase
319 microdomains. The mechanical stress of the plasma membrane caused by antibody binding to
320 raftophilic variable surface antigens then triggers the immediate clearance of the former antigen
321 into extracellular MVs while stimulating antigenic switching. Although the induction of
322 microvesicles by different stress conditions has been observed in many protozoan parasites[38],
323 their association with AV has never been investigated. Our novel observations that the original
324 surface antigen is removed from the plasma membrane into microvesicles suggest that this
325 process may divert the immune response to these MVs to allow the parasite to complete
326 antigenic exchange before increasing concentrations of antibodies agglutinate the cells and/or
327 exceed their endocytic capacity.

328 In the intestinal parasite *G. lamblia*, anti-VSP antibodies may cause not only antigenic
329 switching at early stages of antibody production by the host but also parasite detachment from
330 the gut epithelium when antibody concentrations increase during infections. Due to peristalsis,
331 agglutinated trophozoites can thus reach the lower portions of the small intestine, where they
332 differentiate into cysts[4]. Released cysts containing trophozoites already expressing different
333 VSPs are then prone to reinfect the same individual and to expand the range of potential hosts[8,39].

334 In contrast to *Giardia,* in which higher antibody concentrations favour parasite clumping
335 and thus cell differentiation, increasing concentrations of anti-VSG antibodies may kill most of
336 the bloodstream forms of *T. brucei* before some switchers can proliferate, shaping infections as
337 multi-waves instead of an ever-growing curve expected for a survival strategy. It is known that
338 VSG switching involves enzymes of the phosphoinositol phosphate pathway[40] and that
339 antibodies to VSGs also trigger a cytoplasmic increase of calcium levels[41], suggesting that acidic
340 phospholipids and Ca^{2+} might also be involved during antigenic variation in this parasite.

341   Moreover, antibody-induced switching in *T. brucei* may explain why the *in vivo* dynamics of
342   infections shows a higher VSG diversity than that observed *in vitro*[42] and how antibodies lose
343   their ability to mediate parasite clearance at unexpectedly early stages of VSG coat
344   replacement[43].

345   Since many pathogenic protozoa regulate the expression of a unique variant by post-
346   transcriptional and epigenetic mechanisms[10,44], antibodies might reset these control systems
347   through an increase of intracellular $[Ca^{2+}]$[45,46], which may likely occur occasionally in culture.
348   However, regardless of the mechanisms each pathogen uses to switch its surface antigens, one
349   tempting hypothesis is that the antibody-stimulated release of MVs produces stochastic changes
350   in the cytoplasmic levels of specific molecules in individual cells, resetting the epigenetically
351   controlled antigen-expression program. This possibility might explain the stochastic nature of the
352   switching response as well as the need for an increasing antibody exposure to complete antigenic
353   switching of the whole parasite population[47].

354   In *Tetrahymena* and other free-living protozoa, antigenic variation was shown to occur in
355   response to environmental changes[27]. Therefore, the existence of ARCS in such divergent
356   microorganisms highlights the evolutionary significance of this process for protozoan adaptation
357   from a free-living to a parasitic lifestyle, or vice versa[48].

References

1. Deitsch, K.W., Lukehart, S.A. & Stringer, J.R. Common strategies for antigenic variation by bacterial, fungal and protozoan pathogens. *Nat Rev Microbiol.* **7**, 493–503 (2009). DOI: 10.1038/nrmicro2145

2. Ross, D.T.R. A case of sleeping sickness studied by precise enumerative methods: Regular periodical increase of the parasites disclosed. *Proc. R. Soc. Lond. B.* **82**, 411–415 (1910). DOI: 10.1098/rspb.1910.0035

3. Turner, C.M.R. A perspective on clonal phenotypic (antigenic) variation in protozoan parasites. *Parasitol.* **125**, S17–S23 (2002). DOI: 10.1017/s0031182002002470

4. Adam, R.D. Biology of *Giardia lamblia*. *Clin Microbiol Rev.* **14**, 447–475 (2001). DOI: 10.1128/CMR.14.3.447-475.2001

5. Aggarwal, A. & Nash, T.E. Antigenic variation of *Giardia lamblia in vivo*. *Infect Immun.* **56**, 1420–1423 (1988). DOI: 10.1128/iai.56.6.1420-1423.1988

6. Nash, T.E. & Aggarwal, A. Cytotoxicity of monoclonal antibodies to a subset of *Giardia* isolates. *J Immunol.* **136**, 2628–2632 (1986). https://www.jimmunol.org/content/136/7/2628.long

7. Adam, R.D., Nigam, A., Seshadri, V., Martens, C.A., Farneth, G.A., *et al*. The *Giardia lamblia vsp* gene repertoire: characteristics, genomic organization, and evolution. *BMC Genomics.* **11**, 424 (2010). DOI: 10.1186/1471-2164-11-424

8. Nash, T. E. Antigenic variation in *Giardia lamblia* and the host's immune response. *Phil. Trans. R. Soc. Lond. B.* **352**, 1369–1375 (1997). DOI: 10.1098/rstb.1997.0122

9. Rodríguez-Walker, M., Molina, C.R., Luján, L.A., Saura, A., Bertolotti, V.M., *et al*. Characterization of Cysteine-rich protein families of *Giardia lamblia* and their role during antigenic variation. Preprint at https://biorxiv.org/cgi/content/short/2022.03.07.483299v1

10. Prucca, C.G., Rivero, F.D. & Luján, H.D. Regulation of antigenic variation in *Giardia lamblia*. *Annu Rev Microbiol.* **65**, 611–30 (2011). DOI: 10.1146/annurev-micro-090110-102940

11. Barry, J.D. Capping of variable antigen on *Trypanosoma brucei*, and its immunological and biological significance. *J Cell Sci.* **37**, 287–302 (1979). DOI: 10.1242/jcs.37.1.287

12. Calderón, J., de Lourdes Muñoz, M. & Acosta, H. M. Surface redistribution and release of antibody-induced caps in entamoebae. *J Exp Med.* **151**, 184–193 (1980). DOI: 10.1084/jem.151.1.184

13. Field, M.C. & Carrington, M. The trypanosome flagellar pocket. *Nat Rev Microbiol.* **7**, 775–786 (2009). DOI: 10.1038/nrmicro2221

14. Hoover, D.L., Berger, M., Oppenheim, M.H., Hockmeyer, W.T. & Meltzer, M.S. Cytotoxicity of human serum for *Leishmania donovani* amastigotes: antibody facilitation of alternate complement pathway-mediated killing. *Infect Immun.* **47**, 247–252 (1985). DOI: 10.1128/iai.47.1.247-252.1985

15. Hemphill, A., Stäger, S., Gottstein, B. & Müller, N. Electron microscopical investigation of surface alterations on *Giardia lamblia* trophozoites after exposure to a cytotoxic monoclonal antibody. *Parasitol Res.* **82**, 206–210 (1996). DOI: 10.1007/s004360050096

16. Nash, T. E., Banks, S.M., Alling, D.W., Merritt J.W. & Conrad, J.T. Frequency of variant antigens in *Giardia lamblia*. *Exp Parasitol.* **71**, 415–421 (1990). DOI: 10.1016/0014-4894(90)90067-m

17. Touz, M.C., Rópolo, A.S., Rivero, M.R., Vranych, C.V., Conrad, J.T., *et al*. Arginine deiminase has multiple regulatory roles in the biology of *Giardia lamblia*. *J Cell Sci*. **121**, 2930–2938 (2008). DOI: 10.1242/jcs.026963

18. Touz, M.C., Conrad, J.T. & Nash, T.E. A novel palmitoyl acyl transferase controls surface protein palmitoylation and cytotoxicity in *Giardia lamblia*: VSP palmitoylation. *Mol Microbiol*. **58**, 999–1011 (2005). DOI: 10.1111/j.1365-2958.2005.04891.x

19. Heyworth, M.F. Relative susceptibility of *Giardia muris* trophozoites to killing by mouse antibodies of different isotypes. *J Parasitol*. **78**, 73–76 (1992).

20. Mowatt, M.R., Luján, H.D., Cotten, D.B., Bowers, B., Yee, J., *et al*. Developmentally regulated expression of a *Giardia lamblia* cyst wall protein gene. *Mol Microbiol*. **15**, 955–963 (1995).

21. Luria, S.E. & Delbrück, M. Mutations of bacteria from virus sensitivity to virus resistance. *Genetics*. **28**, 491-511 (1943). DOI: 10.1093/genetics/28.6.49129.

22. Aitcheson, N., Talbot, S., Shapiro, J., Hughes, K., Adkin, C., *et al*. VSG switching in *Trypanosoma brucei*: antigenic variation analysed using RNAi in the absence of immune selection. *Mol Microbiol.* **57**, 1608-22 (2005). DOI: 10.1111/j.1365-2958.2005.04795.x

23. Lawson, E.L., Mills, D.R., Brilliant, K.E. & Hixson, D.C. The transmembrane domain of CEACAM1-4S is a determinant of anchorage independent growth and tumorigenicity. *PLoS One*. **7**, e29606 (2012). DOI: 10.1371/journal.pone.0029606

24. Russ, W.P. & Engelman, D.M. The GxxxG motif: a framework for transmembrane helix-helix association. *J Mol Biol*. **296**, 911–919 (2000). DOI: 10.1006/jmbi.1999.3489

25. Sal-Man, N., Gerber, D., Bloch, I. & Shai, Y. Specificity in transmembrane helix-helix interactions mediated by aromatic residues. *J Biol Chem*. **282**, 19753–19761 (2007). DOI: 10.1074/jbc.M610368200

26. Lorent, J.H. & Levental, I. Structural determinants of protein partitioning into ordered membrane domains and lipid rafts. *Chem Phys Lipids*. **192**, 23–32 (2015). DOI: 10.1016/j.chemphyslip.2015.07.022

27. Simon, M.C. & Schmidt, H.J. Antigenic variation in ciliates: antigen structure, function, expression. *J Eukaryot Microbiol*. **54**, 1–7 (2007). DOI: 10.1111/j.1550-7408.2006.00226.x

28. Mendez, T.L., De Chatterjee, A., Duarte, De Leon, T. J., Robles-Martinez, L., *et al*. Sphingolipids, lipid rafts, and giardial encystation: The show must go on. *Curr Trop Med Rep*. **2**, 136–143 (2015). DOI: 10.1007/s40475-015-0052-0

29. Brown, D.A. Lipid rafts, detergent-resistant membranes, and raft targeting signals. *Physiology (Bethesda)*. **21**, 430–439 (2006). DOI: 10.1152/physiol.00032.2006

30. Einarsson, E., Ástvaldsson, Á., Hultenby, K., Andersson, J.O., Svärd, S.G. & Jerlström-Hultqvist, J. Comparative cell biology and evolution of annexins in diplomonads. *mSphere*. **1** (2016), doi:10.1128/mSphere.00032-15. DOI: 10.1128/mSphere.00032-15

31. Odorizzi, G. The multiple personalities of Alix. *J Cell Sci*. **119**, 3025–3032 (2006). DOI: 10.1242/jcs.03072

32. Henne, W.M., Buchkovich, N. J. & Emr, S. D. The ESCRT pathway. *Dev Cell*. **21**, 77–91 (2011). DOI: 10.1016/j.devcel.2011.05.015

33. Evans-Osses, I., Mojoli, A., Monguió-Tortajada, M., Marcilla, A., Aran, V., *et al*. Microvesicles released from *Giardia intestinalis* disturb host-pathogen response *in vitro*. *Eur J Cell Biol*. **96**, 131–142 (2017). DOI: 10.1016/j.ejcb.2017.01.005

34. Gupta, S., Bromley, J. & Saffarian, S. High-speed imaging of ESCRT recruitment and dynamics during HIV virus like particle budding. *PLoS One*. **15**, e0237268 (2020). DOI: 10.1371/journal.pone.0237268

35. Lizarbe, M., Barrasa, J., Olmo, N., Gavilanes, F. & Turnay, J. Annexin-phospholipid interactions. Functional implications. *Int J Med Sci*. **14**, 2652–2683 (2013). DOI: 10.3390/ijms14022652

36. Rho, S.B., Song, Y.J., Lim, M.C., Lee, S.-H., Kim, B-R. & Park, S-Y. Programmed cell death 6 (PDCD6) inhibits angiogenesis through PI3K/mTOR/p70S6K pathway by interacting of VEGFR-2. *Cell Signal*. **24**, 131–139 (2012). DOI: 10.1016/j.cellsig.2011.08.013

37. Denny, P.W., Field, M.C. & Smith., D.F. GPI-anchored proteins and glycoconjugates segregate into lipid rafts in Kinetoplastida. *FEBS Lett*. **491**, 148–153 (2001). DOI: 10.1016/s0014-5793(01)02172-x

38. Szempruch, A., Dennison, L., Kieft, R., Harrington, JM & Hajduk, S.L. Sending a message: extracellular vesicles of pathogenic protozoan parasites. *Nat Rev Microbiol.* **14,** 669–675 (2016). DOI: 10.1038/nrmicro.2016.110

39. Svärd, S.G., Meng, T.C., Hetsko, M.L., McCaffery, J.M. & Gillin, F.D. Differentiation-associated surface antigen variation in the ancient eukaryote *Giardia lamblia*. *Mol Microbiol*. **30**, 979–989 (1998). DOI: 10.1046/j.1365-2958.1998.01125.x

40. Cestari, I. & Stuart, K. Inositol phosphate pathway controls transcription of telomeric expression sites in trypanosomes. *Proc Natl Acad Sci USA*. **112**, E2803–E2812 (2015). DOI: 10.1073/pnas.1501206112

41. Mendoza, M., Uzcanga, G.L., Pacheco, R., Rojas, H., Carrasquel, L.M., *et al*. Anti-VSG antibodies induce an increase in *Trypanosoma evansi* intracellular Ca^{2+} concentration. *Parasitol*. **135**, 1303–1315 (2008). DOI: 10.1017/S0031182008004903

42. Dubois, M.E., Demick, K.P. & Mansfield, J.M. Trypanosomes expressing a mosaic Variant Surface Glycoprotein coat escape early detection by the immune system. *Infect Immun*. **73**, 2690–2697 (2005). DOI: 10.1128/IAI.73.5.2690-2697.2005

43. Pinger, J., Chowdhury, S. & Papavasiliou, F.N. Variant surface glycoprotein density defines an immune evasion threshold for African trypanosomes undergoing antigenic variation. *Nat Commun*. **8**, 828 (2017). DOI: 10.1038/s41467-017-00959-w

44. Guizetti, J. & Scherf, A. Silence, activate, poise and switch! Mechanisms of antigenic variation in *Plasmodium falciparum. Cell Microbiol*. **15**, 718–726 (2013). DOI: 10.1111/cmi.12115

45. Raynal, N.J-M., Lee, J.T., Wang, Y., Beaudry, A., Madireddi, P., *et al*. Targeting calcium signalling induces epigenetic reactivation of tumour suppressor genes in cancer. *Cancer Res*. **76**, 1494–1505 (2016). DOI: 10.1158/0008-5472.CAN-14-2391

46. Sharma, A., Nguyen, H., Geng, C., Hinman, M.N., Luo, G. & Lou, H. Calcium-mediated histone modifications regulate alternative splicing in cardiomyocytes. Proc Natl Acad Sci USA. **111**, E4920-E4928 (2014). DOI: 10.1073/pnas.140896411

47. Duraisingh, M.T. & Horn, D. Epigenetic regulation of virulence gene expression in parasitic protozoa. *Cell Host & Microbe*. **19**, 629–640 (2016). DOI: 10.1016/j.chom.2016.04.020

48. Xu, F., Jerlström-Hultqvist, J., Kolisko, M., Simpson, A.G.B., Roger, A.J., *et al*. On the reversibility of parasitism: adaptation to a free-living lifestyle via gene acquisitions in the diplomonad *Trepomonas sp*. *BMC Biol*. **14**, 62 (2016). DOI: 10.1186/s12915-016-0284-z

493

Acknowledgments

498

Funding

503

Author contributions

AHT, LAL and DNR contributed the *in vivo* and *in vitro* antigenic switching experiments in
Giardia. LAL and CRM contributed to the generation of mutants, calcium experiments and
fluctuation tests. AT contributed pilot *Giardia* viability, proliferation and switching experiments.
AS generated anti-VSP mAbs and pAbs against *T. brucei* and *T. thermophila*. DOP performed
mAb and antibody fragment purification and quantification. MCS contributed to flow cytometry
experiments. MRW and EAF performed statistical analyses, selected sample sizes and
reanalysed proteomics results and fluctuation tests. PAI, MAB, AHT, LAL, CRM, PRG and
VEA contributed the *T. brucei* experiments; VM and WDS contributed the confocal, scanning
and transmission electron microscopy; JCP validated purified MVs. VEA, WDS and HDL
analysed the data. HDL conceived the project and designed the experiments. AHT, LAL, DNR,
VEA, WDS and HDL wrote the paper. All authors read and made comments on the manuscript.

516

Competing interests

The authors declare no competing interest.

519

Data and materials availability

All data are available in the main text or the supplementary materials. Proprietary antibodies are
available upon request through a material transfer agreement (MTA). The mass spectrometry
proteomics data have been deposited at the ProteomeXchange Consortium via the PRIDE partner
repository with the dataset identifiers PXD031141 and 10.6019/PXD031141 (Reviewer's
account details: Username**:** reviewer_pxd031141@ebi.ac.uk; Password**:** QmM5xe8V).

526

Corresponding author

Correspondence to H.D. Luján (hlujan@ucc.edu.ar).

Figures
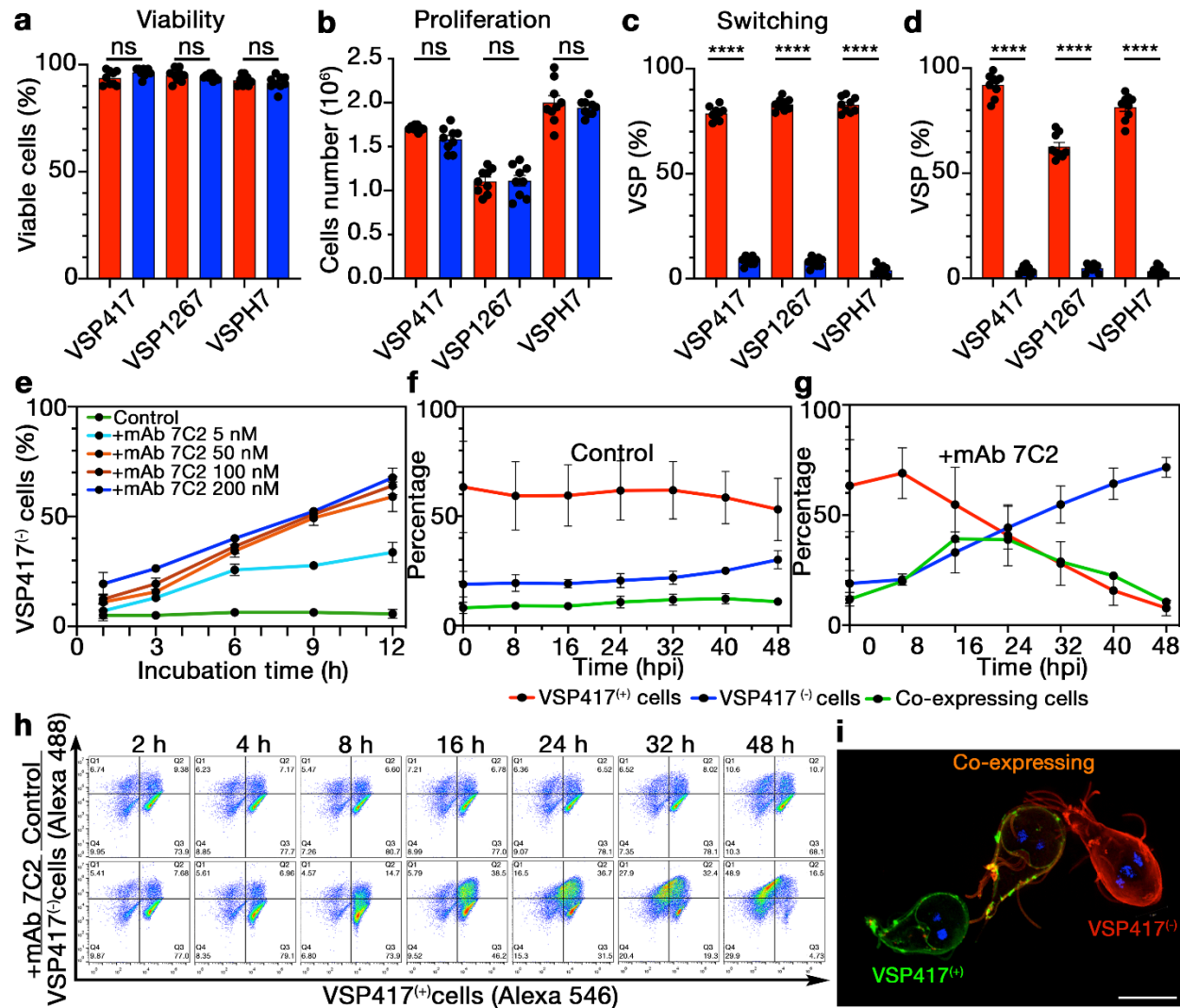
**Figure 1| Antibodies to *Giardia* VSPs stimulate antigenic variation. a-c,** Different VSP clonal populations were grown in the presence of 50 nM of either anti-CWP1 mAb (red columns, controls) or their cognate anti-VSP mAb (blue columns) for 72 h; then, the percentage of live cells (**a**), the total number of cells (**b**) and the percentage of the original VSP in each population (**c**) were determined. **d,** Percentage of cells expressing particular VSPs after *Giardia* cloning in the presence of their cognate anti-VSP mAb (blue) or the control (red). **e,** Percentages of VSP417$^{(-)}$ cells after discrete incubation times with mAb 7C2 at varying concentrations. **f** and **g**, Percentages of VSP417$^{(-)}$, VSP417$^{(+)}$ and co-expressing cells treated with mAb 7C2 (50 nM) for 48 h. **h,** Representative cytograms showing the anti-clockwise distribution shift from VSP417$^{(+)}$ to VSP417$^{(-)}$ cells when cells were stimulated with mAb 7C2 (+ mAb 7C2) at different hpi. Incubation with mAb 8F12 (Control) shows no redistribution. **i,** Super-resolution structured illumination microscopy showing three trophozoites at different stages of antigenic switching after 24 h of mAb stimulation. Scale bar, 5 μm. Values represent mean ± s.e.m. of three independent experiments performed in triplicate. *$p<0.05$; **$p<0.01$; ***$p<0.001$; ****$p<0.0001$; ns, not significant.

14
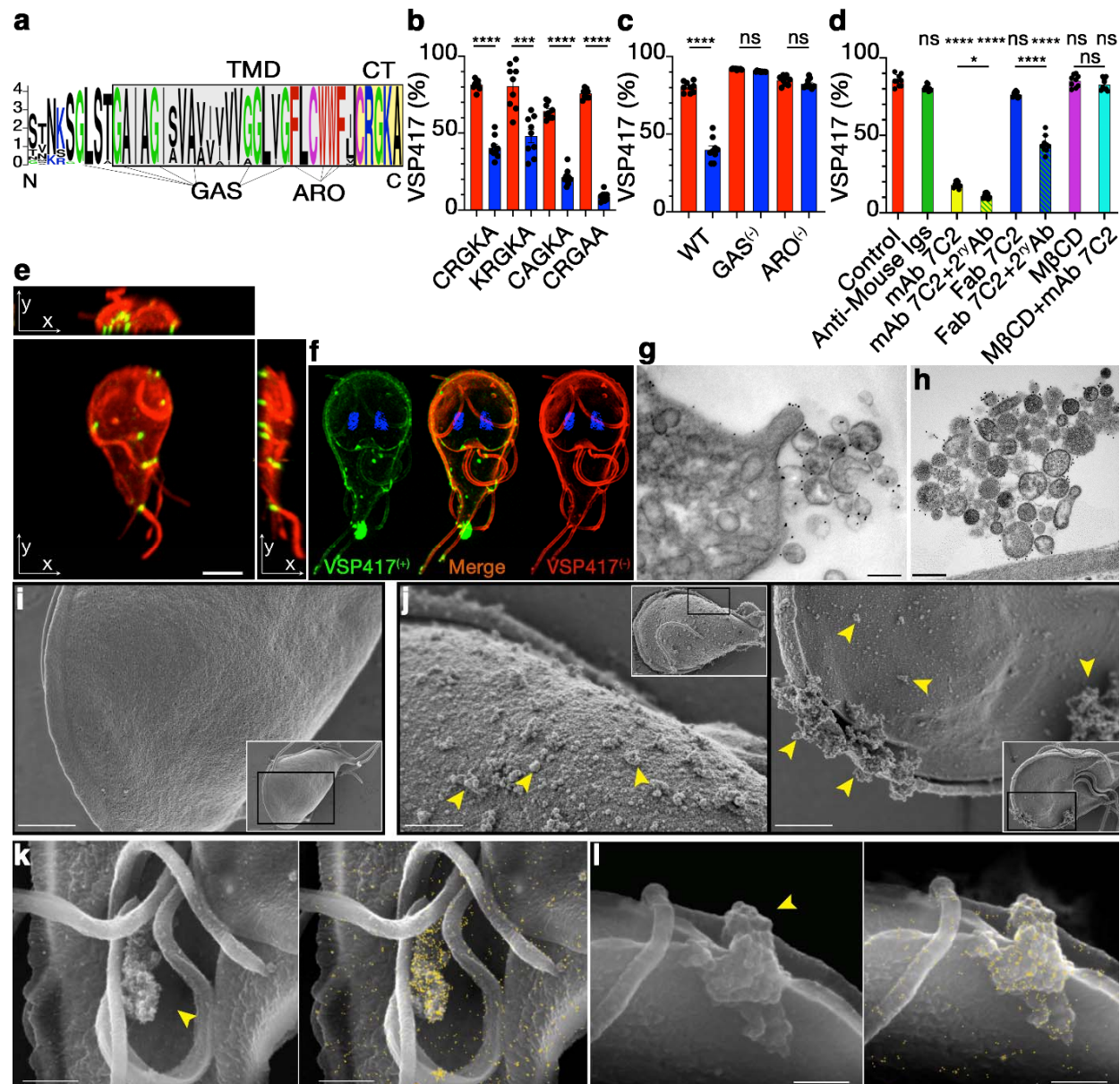
Figure 2| VSP signals through clustering by antibodies. a, Sequence logo of the C-terminus of VSPs. TMD and CT are boxed in grey and yellow, respectively. G-xxx-G and small-xxx-small motifs (GAS) and aromatic residues (ARO) are indicated. **b** and **c,** VSP417 trophozoites coexpressing variants of the CT (b) and the TMD (c) of VSPH7 showing the percentage of VSP417[(+)] cells after 72 h in the presence of either mAb 7C2 (blue) or the control (red). Values were normalized to percentage of cells coexpressing both VSPs. **d**, Percentage of VSP417-expressing cells after 72 h in the presence of mAb 7C2 (50 nM), Fab (100 nM) and Fab in combination with a secondary antibody (2[ry] Ab), and in the presence or absence of MβCD (10 mM). **e**, VSP417-expressing trophozoite after 1 h of treatment with mAb 7C2 (red); then fixed and incubated with mAb 7C2 (green). Maximum intensity projections on the three orthogonal axes from images taken in Z-stack show microdomains of VSP417 bound to the antibody (yellow) and free VSP417 (red). Scale bar 5 µm. **f**, SR-SIM showing colocalization (yellow) of the former VSP (VSP417, green) and the newly expressed VSP (VSP417[(-)], red) after 24 hpi with

15

560   mAb 7C2. **g** and **h**, TEM with gold labelling of a VSPH7 trophozoite incubated for 30 m with
561   mAb G10/4 (g) and of a VSP417 trophozoite incubated for 30 min with mAb 7C2 (h). Scale
562   bars, 500 nm. **i** and **j**, SEM images of a control cell (i) and mAb 7C2-treated trophozoites for 1 h
563   (j). Insets are the cells from which a region (black box) was amplified. Arrowhead shows groups
564   of microvesicles. **k** and **l**, SEM of VSPH7 trophozoites incubated with gold-labelled mAb G10/4
565   for 30 min showing images obtained by secondary (left) and backscattered electrons (right).
566   Arrows indicate groups of microvesicles containing VSPH7/mAb complexes (yellow dots).
567   Scale bar 1 μm. Values represent mean ± s.e.m. of three independent experiments performed in
568   triplicate. *p<0.05; **p<0.01; ***p<0.001. ****p<0.0001; ns, not significant.
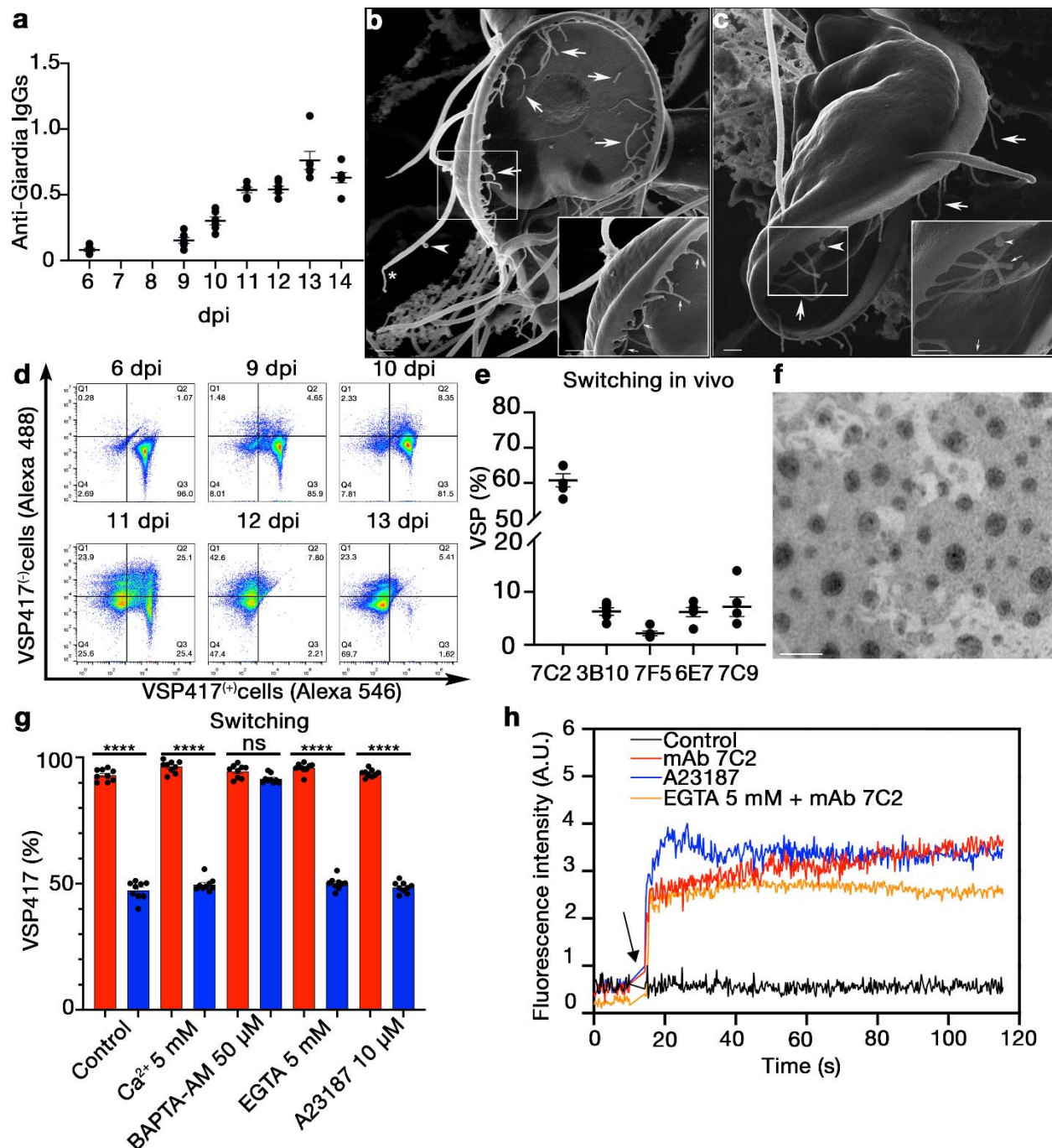
Figure 3| VSPs are released into microvesicles. a, Total antibodies against *Giardia* VSP417-expressing trophozoites detected by ELISA in sera from infected gerbils at different dpi. Values represent relative optical density. **b** and **c**, Extreme Resolution HI-SEM of VSP417 trophozoites recovered from the small intestine at 12 dpi. Extensive membrane projections emerging from the cell flange and the ventral disc are shown (arrows). A vesicle budding from a flagellum (arrowhead) and membrane projections at the end of a flagellum (asterisks) are observed. Scale bar 1 µm. **d**, Representative cytograms showing the distribution shift from VSP417$^{(+)}$ to VSP417$^{(-)}$ populations during animal infections with a VSP417 clone. **e**, Percentage of intestinal trophozoites recognized by different anti-VSP mAbs at 11 dpi. **f**, Negative staining of purified

17

579   microvesicles obtained trophozoites of clone VSP417 incubated with mAb 7C2 for 4 h. Scale

580   bar, 200 nm. **g**, Effects of different concentrations of extracellular calcium, EGTA, BAPTA-AM

581   and the Ca^{2+} ionophore A23187 on antigenic switching of VSP417-expressing trophozoites

582   grown in the presence of a control mAb (red) or of mAb 7C2 (blue) for 72 h. **h**, The effects of

583   anti-VSP mAb 7C2, a control antibody and the calcium ionophore A23187 on the intracellular

584   levels of Ca^{2+} in VSP417-expressing cells are shown. Each line corresponds to the mean value of

585   three independent experiments. Arrow indicates the time at which the stimulus was added.

586   Values in other panels represent mean ± s.e.m. of three independent experiments performed in

587   triplicate. *$p<0.05$; **$p<0.01$; ***$p<0.001$; ****$p<0.0001$; ns, not significant.

Figure 4| ARCS in other protozoa. a-f, HR-SEM micrographs of monomorphic forms *T. brucei* expressing VSG 221a incubated with mouse serum obtained 15 dpi at 1/1,000 dilution (a, 5 mpi, b-f, 4 hpi). Extensive membrane projections emerging from the cell surface and large amounts of microvesicles can be observed (arrowheads). Scale bars 1 µm. **g**, Induction of switching by three daily additions of anti-VSG antibodies in *T. brucei* clone EATRO1125 expressing VSG AnTat1.1, following the protocol depicted in Extended Data Fig. 6. After 72 h, non-switchers were killed with a lethal antibody dilution (1/50) and switchers were selected at random in each plate for their identification (the first number or letter of the ID code indicates the plate: control; 1 dose; 2 doses; 3 doses; the following letter and number indicate the position within the plate) along with the identified VSG and a unique colour code for each VSG. Wells in which the VSG was not identified are in grey. **h-j**, HR-SEM micrographs of *T. thermophila* cells untreated (**h**) or treated with an antiserum directed to their variable surface antigens after 4 hpi (**i, j**). Insets correspond to the whole cells and the amplified image is denoted by black boxes. A massive

602   release of microvesicles still attached to the cell surface can be observed in treated cells, which is
603   not seen in the controls. Scale bars 2 µm.